Waves Random Media **10** (2000) 381–394. Printed in the UK PII: S0959-7174(00)12591-1

Statistical moments of travel times at second order in isotropic and anisotropic random media

B Iooss†, Ph Blanc-Benon‡ and C Lhuillier†

† CEA Cadarache, DRN/DER/SSAE/LSMN, 13108 St Paul lez Durance, France
‡ Laboratoire de Mécanique des Fluides et d'Acoustique, URA CNRS 5509, Ecole Centrale de Lyon, BP 163, 69131 Ecully Cedex, France

E-mail: iooss@cervoise.cad.cea.fr, christian.lhuillier@cea.fr and Philippe.Blanc-Benon@ec-lyon.fr

Received 14 March 2000

Abstract. We study the high-frequency propagation of acoustic plane and spherical waves in random media. With the geometrical optics and the perturbation approach, we obtain the travel-time mean and travel-time variance at the second order. The main hypotheses are the Gaussian distribution of the acoustic speed perturbation and a factorized form for its correlation function. The second-order travel-time variance explains the nonlinear behaviour at large propagation distance observed with numerical experiments based on ray tracing. Usually, homogeneity and isotropy of the refractive index are considered. Using the geometrical anisotropy hypothesis we extend the theory to a general class of statistically anisotropic random media.

1. Introduction

The theory of wave propagation in turbulent media is founded on the statistical representation of isotropic and homogeneous turbulence (Tatarskii [25]). High-frequency propagation in random media has been studied extensively, and there exists a vast amount of literature on the subject. The basic theory considered a plane wave in an isotropic and homogeneous random medium (Chernov [5]) or in a locally isotropic and homogeneous random medium (Tatarskii [25]). To make the statistical inference possible, waves have to meet many heterogeneities during their propagation. This condition is expressed by

$$L \ll X \tag{1}$$

where X is the propagation distance and L is the characteristic length of the inhomogeneities.

The modern theory of wave propagation in random media uses the parabolic approximation to connect fluctuations of a plane or spherical wave to medium variations (Rytov *et al* [20]). The parabolic approximation neglects backscattering by assuming a dominant wavelength λ which is shorter than the heterogeneities sizes:

$$\lambda \ll L. \tag{2}$$

On one hand, with an additional Markovian hypothesis, we are able to study statistical moments of the full wavefield; on the other hand, the Rytov approximation permits one to deal with log amplitude and arrival time fluctuations. The Rytov approximation is valid provided the wavefield fluctuations are smooth, which means that diffraction effects are small (Rytov *et al* [20], Shapiro *et al* [23], Samuelides [21]).

0959-7174/00/030381+14$30.00

One of the effects of random heterogeneities is the velocity shift effect which states that the apparent velocity of the wave is larger than the average velocity of the medium. This is in accordance with Fermat's principle: the wave path minimizes the travel time of the wave. Theoretically, this can be explained by a second-order derivation of the average travel time (Roth *et al* [19], Samuelides and Mukerji [22], Samuelides [21]).

Another well known effect is the linear increase of the first-order travel-time variance with the propagation distance (Chernov [5]). However, nonlinear effects appear at a certain propagation distance (Karweit *et al* [13]). This phenomenon is closely related to the occurrence of first caustics (Kulkarny and White [17], Blanc-Benon *et al* [1, 2]).

In this paper, we are concerned with the travel time in its natural domain of validity: the geometrical optics theory, which neglects all diffraction phenomena. In the next section, general model and travel-time expressions are given. Therefore, we present the development at the second order of the travel-time mean and variance in isotropic media. To validate our result on the travel-time variance, we compare theoretical predictions and numerical results obtained by the ray tracing and the Gaussian beam summation methods. In the final section, we extend the formulae to a well known class of anisotropic model in geostatistics: the geometrical anisotropy.

2. Travel times in random media

We consider the propagation of monochromatic acoustic waves, which satisfy the Helmholtz equation, in an inhomogeneous motionless medium: $u(\boldsymbol{r}, t) = u(\boldsymbol{r})\,\mathrm{e}^{-\mathrm{i}\omega_0 t}$, where u is the wavefield, $\boldsymbol{r}$ the point location, t the time and ω_0 the acoustic frequency. In the high-frequency regime, the wavefield $u(\boldsymbol{r})$ in a random medium is a random function with fluctuations of its travel time $T(\boldsymbol{r})$ and amplitude $A(\boldsymbol{r})$: $u(\boldsymbol{r}) = A(\boldsymbol{r})\,\mathrm{e}^{\mathrm{i}\omega_0\, T(\boldsymbol{r})}$.

A rigorous consideration of the travel times requires the geometrical optics approximation. In the geometrical optics, diffraction phenomena are ignored because the size of the first Fresnel zone is much smaller than the transverse scale length of heterogeneities $l_\perp$:

$$\sqrt{\lambda X} \ll l_\perp. \tag{3}$$

Therefore, the travel time satisfies the eikonal equation $[\nabla T(\boldsymbol{r})]^2 = \frac{1}{c^2(\boldsymbol{r})}$, where c is the acoustic speed. Moreover, we suppose that $\frac{1}{c^2(\boldsymbol{r})}$ deviates only weakly from a constant value and we write

$$[\nabla T(\boldsymbol{r})]^2 = \frac{1}{c^2(\boldsymbol{r})} = \frac{1}{c_0^2}[1 + \epsilon(\boldsymbol{r})] \tag{4}$$

where c_0 is a constant acoustic speed and ϵ are small fluctuations ($|\epsilon| \ll 1$).

We expand T as a power series in the small perturbation parameter ϵ. Keeping terms up to the second order gives $T(\boldsymbol{r}) = T_0 + T_1(\boldsymbol{r}) + T_2(\boldsymbol{r})$. Let $\boldsymbol{r} = (r_\parallel, \boldsymbol{r}_\perp)$ be a vector in the propagation basis ($(r_\parallel, 0)$ is oriented along the propagation direction) and let X be the propagation distance (see figure 1). For a spherical wave, the different terms contributing to the travel time are expressed as

$$T_0(\boldsymbol{r}) = \frac{\|\boldsymbol{r}\|}{c_0} = \frac{X}{c_0} \tag{5}$$

$$T_1(\boldsymbol{r}) = \frac{1}{2c_0}\int_{\boldsymbol{r}} \epsilon(\boldsymbol{r}')\,\mathrm{d}\boldsymbol{r}' = \frac{1}{2c_0}\int_0^X \epsilon(r', \boldsymbol{r}_\perp)\,\mathrm{d}r' \tag{6}$$

$$T_2(\boldsymbol{r}) = -\frac{1}{4c_0}\int_0^X \left[\int_0^{r'} \frac{r''}{r'} \nabla_\perp \epsilon(r'', \boldsymbol{r}_\perp)\,\mathrm{d}r''\right]^2 \mathrm{d}r'. \tag{7}$$

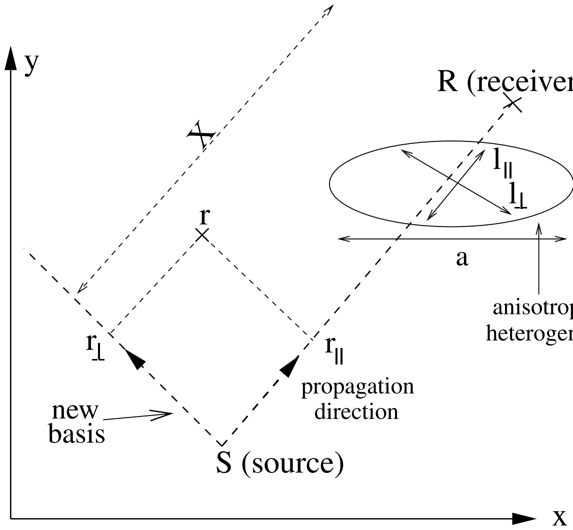

Figure 1. Geometry of the problem, graphical illustration of the anisotropy: the horizontal a, vertical b, parallel $l_{\|}$ and transverse $l_{\perp}$ correlation lengths.

For a plane wave, expressions are similar except for T_2 where $\frac{r''}{r'} = 1$.

T_0 is the deterministic term corresponding to a constant speed medium, which leads to a straight ray. T_1 gives the first-order fluctuations by integrating medium perturbations along the straight ray. T_2 describes the leading-order effect of the ray bending due to perturbations (Snieder and Aldridge [24]). It has been given for spherical waves by Boyse and Keller [3].

When ray bending increases, stronger nonlinear travel-time perturbations appear, and higher-order terms must be taken into account (Snieder and Aldridge [24]).

3. The isotropic case

3.1. The random models

Let us suppose that $\epsilon(\boldsymbol{r})$ is a weak and centred random field: $|\epsilon| \ll 1$, $\langle\epsilon\rangle = 0$. If $c(\boldsymbol{r})$ is the acoustic speed, we obtain by linearization of equation (4):

$$c(\boldsymbol{r}) = c_0\left[1 - \tfrac{1}{2}\epsilon(\boldsymbol{r})\right] \tag{8}$$

where c_0 is the average acoustic speed ($\langle c\rangle = c_0$). To make statistical inference possible, we suppose that ϵ is statistically homogeneous. Therefore, ϵ is defined by its autocorrelation function (or covariance) $C_\epsilon(\boldsymbol{r}) = \langle\epsilon(\boldsymbol{r}+\boldsymbol{r}_1)\epsilon(\boldsymbol{r}_1)\rangle$, where $\boldsymbol{r}$ and $\boldsymbol{r}_1$ are two point locations.

With the additional hypothesis of isotropy, the correlations of ϵ are independent by rotation, then $C_\epsilon(\boldsymbol{r}) = C_\epsilon(\|\boldsymbol{r}\|)$. We define a new function, called the standardized covariance N:

$$C_\epsilon(\boldsymbol{r}) = C_\epsilon(x, y, z) = \sigma_\epsilon^2 N\left(\frac{\|\boldsymbol{r}\|}{L}\right) \tag{9}$$

which has a standard deviation and a correlation length normalized to unity. Finally, a few statistical parameters describe ϵ: its standard deviation $\sigma_\epsilon = \sqrt{\langle\epsilon^2(\boldsymbol{r})\rangle}$, its correlation length L which is a typical size of the heterogeneities, and its standardized covariance N.

To calculate statistical moments of T_2, we will use two parameters which depend on the covariance structure N:

$$A_1 = \int_0^\infty N(u)\,\mathrm{d}u \qquad A_2 = \int_0^\infty \frac{N'(u)}{u}\,\mathrm{d}u \tag{10}$$

where N' is the derivative of N. Let us evaluate the coefficients A_1 and A_2 for different covariance functions.

- The Gaussian covariance $N(h) = \exp(-h^2)$ leads to media with very smooth fluctuations, with only one scale of inhomogeneity: the correlation length. In this case, we have $A_1 = \frac{1}{2}\sqrt{\pi}$ and $A_2 = -\sqrt{\pi}$.
- The exponential covariance $N(h) = \exp(-h)$ models rough models, with a slow decrease of the correlations (as a function of h). For this model, $A_1 = 1$ and A_2 is undefined: our approach will be not valid.
- The spectral density $\Phi(k)$ of a random medium is the Fourier transform of its covariance. The power spectrum $\Phi(k) \propto (1 + k^2L^2)^{-p-3/2}$ $(p \in [0, 1])$ is a generalization of the Kolmogorov spectrum ($\Phi(k) \propto k^{-11/3}$). The Kolmogorov spectrum models the energy cascade in a turbulent fluid (Tatarskii [25]) between the external range L (energy production scale) and the inertial range l_0 (dissipation scale). Therefore, this spectrum is defined for

$$\frac{2\pi}{L} \ll k \ll \frac{2\pi}{l_0}$$

and the power spectrum for $k \ll \frac{2\pi}{l_0}$.
The power spectrum leads to a covariance of the form

$$N(h) = \frac{2^{1-p}}{\Gamma(p)} h^p K_p(h)$$

where K_p is the modified Bessel function of second type and of order p. This model gives

$$A_1 = \frac{\sqrt{\pi}\,\Gamma(\frac{1}{2} + p)}{\Gamma(p)}$$

and

$$A_2 = \frac{\sqrt{\pi}[(-1 + 2p)\Gamma(-\frac{1}{2} + p) + 2\Gamma(\frac{1}{2} + p)]}{4\Gamma(p)}.$$

Therefore, A_2 is defined for $p > \frac{1}{2}$. The case $p = \frac{1}{2}$ corresponds to the exponential covariance.
- The modified Von Karman model is derived from the power model by taking $p = \frac{1}{3}$. To take into account the small inhomogeneities, it introduces in the spectrum a Gaussian filter $\exp(-k^2/k_m^2)$ where $k_m = \frac{5.92}{l_0}$ is a cut-off frequency. The modified Von Karman covariance is written as

$$C(h) = 1.685 C_n^2 k_m^{-2/3} \left[{}_1F_1\left(-\tfrac{1}{3}; \tfrac{3}{2}; -\tfrac{1}{4}k_m^2 h^2\right)\right]$$

where C_n is a constant and $({}_1F_1)$ is the confluent hypergeometric function. Therefore, we take

$$N(h) = {}_1F_1\left(-\tfrac{1}{3}; \tfrac{3}{2}; -\tfrac{1}{4}k_m^2 h^2\right)$$

and we obtain, $A_1 = \frac{2.583}{k_m}$ and $A_2 = \frac{1.076}{k_m}$.

3.2. Travel-time mean and variance

We denote by T^P and T^S the travel times of a plane and of a spherical wave. At first order, the travel time mean is zero because $\langle\epsilon\rangle = 0$ (see equation (6)). The average travel time at second order is deduced from equation (7) and the derivation is given in appendix A. We obtain

$$\langle T(\boldsymbol{r})\rangle = T_0(\boldsymbol{r}) + \langle T_2(\boldsymbol{r})\rangle \tag{11}$$

$$\langle T_2^P(\boldsymbol{r})\rangle = 3\langle T_2^S(\boldsymbol{r})\rangle = \frac{A_2}{8}\frac{\sigma_\epsilon^2}{c_0}\frac{X^2}{L}. \tag{12}$$

For the variance, $\mathrm{Var}(T) = \mathrm{Var}(T_1+T_2) = \langle(T_1+T_2)^2\rangle - \langle T_1+T_2\rangle^2 = \mathrm{Var}(T_1)+\mathrm{Var}(T_2)+\langle T_1T_2\rangle$. The travel-time variance at first order $\mathrm{Var}(T_1)$ is a well known result called the Chernov prediction (Chernov [5], Keller [14]). With the hypothesis of a Gaussian distribution for ϵ, $\langle T_1T_2\rangle = 0$ because this term contains the third-order moment of ϵ which is zero in the Gaussian case. The derivation of the travel-time variance at second order $\mathrm{Var}(T_2)$ is made in appendix B. We obtain

$$\mathrm{Var}[T(\boldsymbol{r})] = \mathrm{Var}[T_1(\boldsymbol{r})] + \mathrm{Var}[T_2(\boldsymbol{r})] \tag{13}$$

$$\mathrm{Var}[T_1^P(\boldsymbol{r})] = \mathrm{Var}[T_1^S(\boldsymbol{r})] = \frac{A_1}{2}\frac{\sigma_\epsilon^2}{c_0^2}LX = \frac{A_1}{2}\frac{\sigma_\epsilon^2}{c_0^2}L^2\frac{X}{L} \tag{14}$$

$$\mathrm{Var}[T_2^P(\boldsymbol{r})] = 9\,\mathrm{Var}[T_2^S(\boldsymbol{r})] = \frac{A_2^2}{32}\frac{\sigma_\epsilon^4}{c_0^2}\frac{X^4}{L^2} = \frac{A_2^2}{32}\frac{\sigma_\epsilon^4}{c_0^2}L^2\left(\frac{X}{L}\right)^4. \tag{15}$$

Therefore, neglecting $\mathrm{Var}(T_2)$ with respect to $\mathrm{Var}(T_1)$ leads to the explicit condition

$$\begin{aligned} &X \ll AL\sigma_\epsilon^{-2/3} \\ &A = 2\left(\frac{2A_1}{A_2^2}\right)^{1/3} \qquad \text{(plane wave)} \\ &A = 2\left(\frac{18A_1}{A_2^2}\right)^{1/3} \qquad \text{(spherical waves).} \end{aligned} \tag{16}$$

For a Gaussian covariance, $A \simeq 1.653$ for a plane wave and $A \simeq 3.438$ for a spherical one. Note that relation (16) provides an estimate of the validity of the asymptotic series in terms of the distance of propagation X with respect to L and σ_ϵ.

3.3. Connection with the probability density of the occurrence of caustics

As an example let us consider an isotropic random medium characterized by a Gaussian covariance. In figure 2, we compared the second-order travel-time variances of plane waves $\mathrm{Var}[T_2^P(\boldsymbol{r})]$, and of spherical waves $\mathrm{Var}[T_2^S(\boldsymbol{r})]$ both with the first-order Chernov estimates. The travel-time variances are plotted in terms of the normalized distance X/L. These comparisons are done for $\sigma_\epsilon = 0.01$ and two values of the correlation length L: $L = 1$ and 0.5 m. We clearly observed that the departures from the Chernov prediction increase with travel distance. The conditions (16) become $\frac{X}{L} \ll 35$ for the plane wave case, and $\frac{X}{L} \ll 74$ for the spherical wave case. We observe visually that the nonlinearity effects due to the second-order term $\mathrm{Var}(T_2)$ appear at a shorter distance and increase much faster in the plane wave case than in the spherical wave case. Indeed, caustics appear at shorter distances for plane waves than for spherical waves (Kulkarny and White [17]). The effect of travel distance has been observed previously by Juvé *et al* [11] for transmission of acoustic waves through two-dimensional (2D) isotropic turbulence and by Karweit *et al* [13] for three-dimensional (3D) random velocity fields. The reason for this behaviour seems to be directly linked to the existence

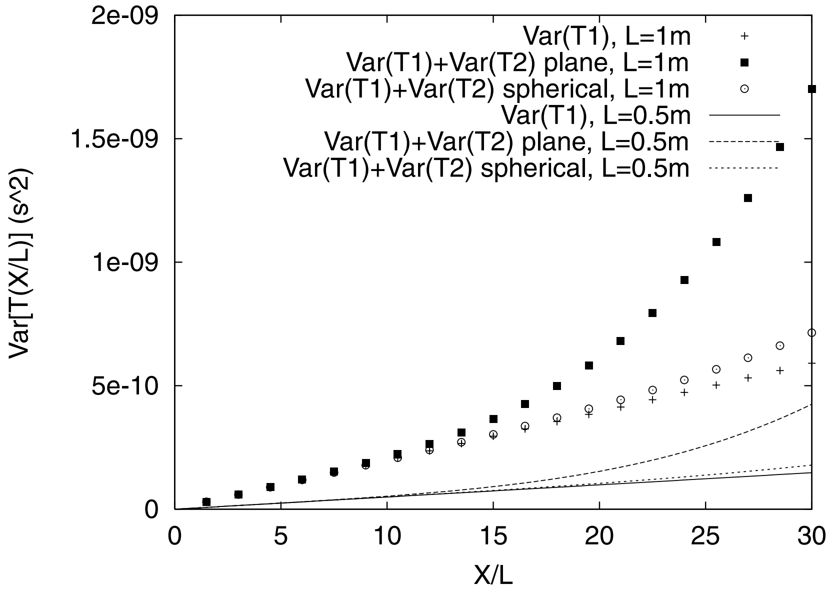

Figure 2. Theoretical travel-time variances versus normalized distance X/L. Curves are plotted for a Gaussian covariance with two scales L(1 m; 0.5 m), a velocity $c_0 = 1500$ m s^{-1} and $\sigma_\epsilon = 0.01$.

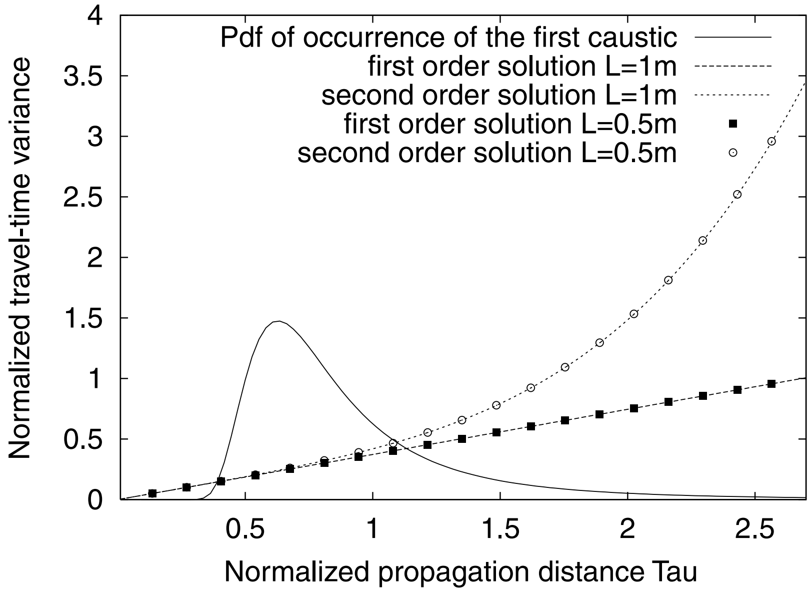

Figure 3. Illustration of the connection between the occurrence of the first caustic and the nonlinear evolution of the travel-time variance. Curves are plotted in the case of a plane wave ($c_0 = 1500$ m s^{-1}, ϵ has a Gaussian covariance, $\sigma_\epsilon = 0.01$, $L = 1$ and 0.5 m).

of caustics. To consolidate this point of view, we plot in figure 3 the probability density of the occurrence of the first caustics as a function of a normalized distance of propagation τ.

For an initially plane wave propagating through 3D isotropic turbulence the probability density $P_3(\tau)$ is defined as

$$P_3(\tau) = \frac{\alpha}{\tau^4} \exp(-\beta/\tau^3) \tag{17}$$

where the coefficients α and β have the values 0.87 and 0.33, respectively. The normalized distance τ is defined by

$$\tau = \mathcal{D}_{3c}^{1/3}\, x \tag{18}$$

where $\mathcal{D}_{3c}$ is the diffusion coefficient introduced by Klyatskin [15]. For a Gaussian correlation function, the diffusion coefficient $\mathcal{D}_{3c}$ is given by (see Blanc-Benon *et al* [2]):

$$\mathcal{D}_{3c} = \frac{\sqrt{\pi}}{2L^3}\, \sigma_\epsilon^2. \tag{19}$$

In figure 3, we plot the travel-time variance normalized by the value of the travel-time variance evaluated at the maximum distance of propagation $X_{\max}$ using the Chernov approximation:

$$\frac{\mathrm{Var}[T_1^P(X)] + \mathrm{Var}[T_2^P(X)]}{\mathrm{Var}[T_1^P(X_{\max})]} = \frac{X}{X_{\max}}\left(1 + \frac{1}{16}\frac{A_2^2}{A_1}\sigma_\epsilon^2 \frac{X^3}{L^3}\right) = \frac{\tau}{\tau_{\max}}\left(1 + \tfrac{1}{4}\tau^3\right). \tag{20}$$

We plot the travel-time variance calculated for two values of L (1 and 0.5 m), and as expected the values are the same. We can also note that for $\tau \leqslant 0.4$ the contribution of the second-order term makes no difference in the evaluation of the travel-time variance, then the influence of the second-order term becomes significant and we note an increase of the travel-time variance. For the probability density for the occurrence of caustics we clearly observed three regimes.

(a) For $\tau \leqslant 0.4$ the value of the PDF is 0, no caustics occurs.
(b) For $0.4 \leqslant \tau \leqslant 2$ the first caustic will occur. The peak of the probability density function appears at a normalized distance τ equal to $(\frac{3}{4}\beta)^{1/3} \cong 0.5994$ (i.e. $X = (\frac{3}{4\mathcal{D}_{3c}}\beta)^{1/3}$). The nonlinear behaviour of the travel-time variance starts just after this peak.
(c) For $\tau \geqslant 2$ the PDF of occurrence of the first caustic goes to 0.

With our value $\sigma_\epsilon = 0.01$, the maximum value of the probability density is obtained when $\frac{X_p}{L} \simeq 14.1$. This is in agreement with the validity condition (16) of the first-order approximation of the travel-time variance which gives an upper limit $\frac{X}{L} \ll 35$.

3.4. A numerical experiment

The effect of the travel-time shift $\langle T_2 \rangle$ between $\langle T \rangle$ and T_0 has been observed by numerous authors. Usually, they work on velocity shifts: because of the fast path effect, the effective velocity is higher than the mean velocity of the medium. Indeed, A_2 is negative, then $\langle T \rangle \leqslant T_0$ and $\frac{X}{\langle T \rangle} \geqslant \frac{X}{T_0}$ (see equation (12)). Theoretical and numerical comparisons are done with plane wave experiments and the agreements are generally good (Roth *et al* [19], Witte *et al* [27], Samuelides and Mukerji [22]).

The nonlinear behaviour of the travel-time variance has been observed by Karweit *et al* [13] and other authors, but has never been compared with a theoretical prediction. With this goal, we have performed synthetic tests. The followed method uses the random Fourier modes for generating random fields (Kraichnan [16], Karweit *et al* [13]), and the Gaussian beam summation to calculate the acoustic field propagated in the medium (Cerveny *et al* [4], Fiorina [6]). The Gaussian beam approach solves the wave equation in the neighbourhood of the conventional rays using the parabolic approximation. The solution associates with each ray

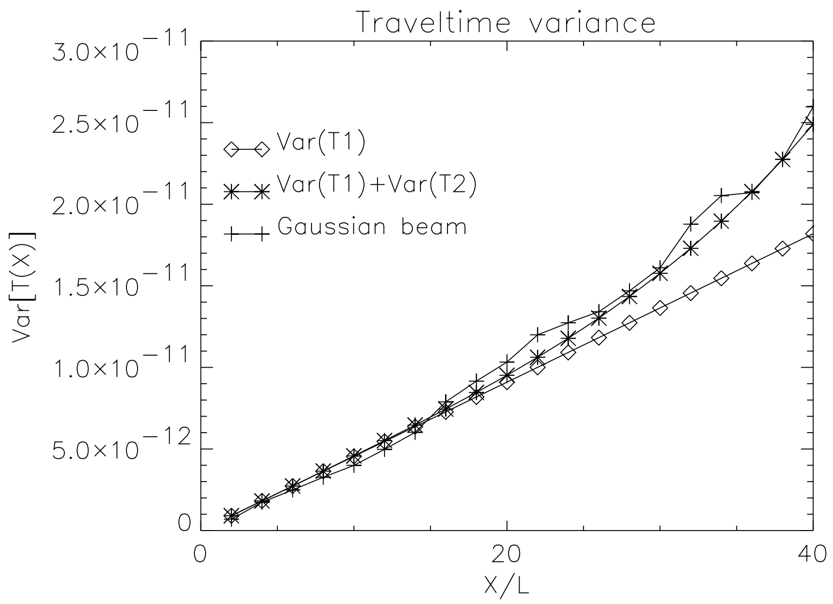

Figure 4. Comparison between theoretical and numerically computed travel-time variances (in s^2).

a beam having a Gaussian amplitude normal to the ray. The solution for a given source is then constructed by a superposition of Gaussian beams along nearby rays. The rays are given from the standard ray-tracing technique, but the use of Gaussian beams has the advantage of avoiding eigenray computations to find the travel times at fixed receivers.

The acoustic velocity has an isotropic Gaussian covariance with $L = 0.1$ m, $\sigma_\epsilon = 0.0038$, $c_0 = 1509.13$ m s^{-1}, and we perform 400 different realizations. The medium has a width of 4 m and a height of 1 m. In each realization, we consider a spherical wave. The source is located at (0; 0.5), the global propagation direction is horizontal, and 201 rays are regularly launched in an opening angle of 10°. 20 receivers are regularly placed on the horizontal axis each 0.2 m spacing, with 0.2 m $\leqslant X \leqslant$ 4 m where X is the propagation distance.

In figure 4, we compare numerical results with theoretical curves: the Chernov solution

$$\mathrm{Var}(T_1) = \frac{\sqrt{\pi}}{4}\frac{\sigma_\epsilon^2}{c_0^2}LX$$

and the new solution

$$\mathrm{Var}(T_1) + \mathrm{Var}(T_2) = \frac{\sqrt{\pi}}{4}\frac{\sigma_\epsilon^2}{c_0^2}LX + \frac{\pi}{288}\frac{\sigma_\epsilon^4}{c_0^2}\frac{X^4}{L^2}.$$

We observe that the nonlinear behaviour is correctly predicted by the new solution.

4. Extension to geometrically anisotropic media

The isotropy hypothesis breaks down in a lot of concerned media, e.g. in the middle atmosphere for radiophysical studies (Rytov *et al* [20]), in the ocean (Flatté *et al* [7]), in 3D turbulent flows (Karweit and Blanc-Benon [12]), in sedimentary basins for the seismic exploration problem

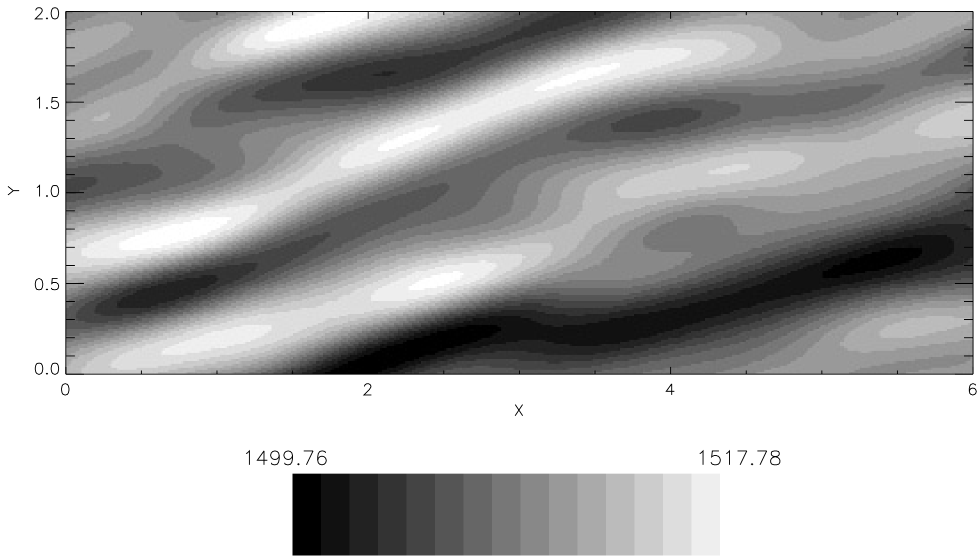

Figure 5. Example of a statistically anisotropic velocity field (axis in metres). The velocity has a Gaussian covariance, with $c_0 = 1509$ m s^{-1}, $\langle c^2 \rangle = 16$ (m s^{-1})^2, $\theta = 11.5°$, $a = 1$ m, $b = 0.25$ m.

(Iooss [9, 10], Samuelides and Mukerji [22]), in the lithosphere and asthenosphere for the seismological framework (Flatté and Wu [8]), etc.

In a 3D anisotropic random medium, instead of having a single correlation length a (which is a measure of the typical heterogeneity size), three correlation lengths a, b and c are needed. Therefore, the refractive index covariance $C(x, y, z)$ cannot be reduced to $C(r)$ with $r = \sqrt{x^2 + y^2 + z^2}$ as in the isotropic case. To simplify the problem, we work with a 2D geometry throughout this section. The extension to 3D is given in appendix C.

4.1. The geometrical anisotropy hypothesis

We assume that ϵ is stationary at second order, with an anisotropic covariance $C_\epsilon(x, y)$ of geometrical type (Wackernagel [26]):

$$C_\epsilon(x, y) = \sigma_\epsilon^2 N \left[\sqrt{\frac{(x\cos\theta + y\sin\theta)^2}{a^2} + \frac{(x\sin\theta - y\cos\theta)^2}{b^2}} \right] \tag{21}$$

where σ_ϵ^2 is the variance of the fluctuations, N the standardized covariance (the statistical structure), θ the stratification angle (with the horizontal axis), a the correlation length in the θ direction and b the correlation length in the normal direction of θ. We admit that the correlation lengths are measures of the heterogeneity scales.

In real problems, taking into account such an anisotropy is important; e.g. the seismic heterogeneities are often strongly stratified and gently sloping; in the atmosphere or in the ocean, the wind or current direction can lead to inadequacy between the propagation direction and the anisotropy axis; in industrial problems (such as pipe flows of a fluid), particular geometries provoke inclined heterogeneities stratification. A random medium with inclined stratification is shown in figure 5.

For wavefield propagation in such media, the correlation lengths of interest are those parallel ($l_\parallel$) and transverse ($l_\perp$) to the propagation direction (see figure 1). We consider $\boldsymbol{r}$

oriented along the principal propagation direction, which forms an angle α with the horizontal axis. Then $\boldsymbol{r} = (r\cos\alpha, r\sin\alpha)$ and we can write

$$C_\epsilon(\boldsymbol{r}) = \sigma_\epsilon^2 N\left[\sqrt{\frac{r^2}{a^2}(\cos\alpha\cos\theta + \sin\alpha\sin\theta)^2 + \frac{r^2}{b^2}(\cos\alpha\sin\theta - \sin\alpha\cos\theta)^2}\right]. \tag{22}$$

In the propagation direction $C_\epsilon(\boldsymbol{r}) = \sigma_\epsilon^2 N(\frac{r}{l_\parallel})$, and we deduce the parallel correlation length $l_\parallel$. In the orthogonal direction, $C_\epsilon(-r\sin\alpha, r\cos\alpha) = \sigma_\epsilon^2 N(\frac{r}{l_\perp})$, and we find the transverse correlation length $l_\perp$. We obtain

$$\begin{aligned} \frac{1}{l_\parallel^2} &= \frac{(\cos\alpha\cos\theta + \sin\alpha\sin\theta)^2}{a^2} + \frac{(\cos\alpha\sin\theta - \sin\alpha\cos\theta)^2}{b^2} \\ \frac{1}{l_\perp^2} &= \frac{(-\sin\alpha\cos\theta + \cos\alpha\sin\theta)^2}{a^2} + \frac{(\sin\alpha\sin\theta + \cos\alpha\cos\theta)^2}{b^2}. \end{aligned} \tag{23}$$

In the example of figure 5 ($a = 1, b = 0.25, \theta = 11.5°$), if we study a horizontal wave ($\alpha = 0$), we obtain $l_\parallel \simeq 0.792$ and $l_\perp \simeq 0.255$.

Finally, on the basis of the wave propagation direction, we have

$$C_\epsilon(\boldsymbol{r}) = C_\epsilon(r_\parallel, r_\perp) = \sigma_\epsilon^2 N\left[\sqrt{\frac{r_\parallel^2}{l_\parallel^2} + \frac{r_\perp^2}{l_\perp^2}}\right]. \tag{24}$$

If $\alpha = \theta = 0$ and $a = b$, we return to the isotropic model with $l_\parallel = l_\perp = a = b$ and $C_\epsilon(\boldsymbol{r}) = \sigma_\epsilon^2 N(\frac{r}{a})$ where $r = \|\boldsymbol{r}\|$.

4.2. Statistical moments of travel times

As in the isotropic case, we start from equations (6) and (7). The main difference in the theoretical derivations is for formula (9). From (24), we obtain

$$\nabla_\perp^2 C_\epsilon(X, r_\perp)|_{r_\perp=0} = \frac{\sigma_\epsilon^2}{X}\frac{l_\parallel}{l_\perp^2}N'\left(\frac{X}{l_\parallel}\right). \tag{25}$$

Therefore, the same techniques than in appendices A and B lead to

$$\langle T_1^P(\boldsymbol{r})\rangle = \langle T_1^S(\boldsymbol{r})\rangle = 0 \tag{26}$$

$$\langle T_2^P(\boldsymbol{r})\rangle = 3\langle T_2^S(\boldsymbol{r})\rangle = \frac{A_2}{8}\frac{\sigma_\epsilon^2}{c_0}\frac{l_\parallel}{l_\perp^2}X^2 \tag{27}$$

$$\mathrm{Var}[T_1^P(\boldsymbol{r})] = \mathrm{Var}[T_1^S(\boldsymbol{r})] = \frac{A_1}{2}\frac{\sigma_\epsilon^2}{c_0^2}l_\parallel X \tag{28}$$

$$\mathrm{Var}[T_2^P(\boldsymbol{r})] = 9\,\mathrm{Var}[T_2^S(\boldsymbol{r})] = \frac{A_2^2}{32}\frac{\sigma_\epsilon^4}{c_0^2}\frac{l_\parallel^2}{l_\perp^4}X^4. \tag{29}$$

Neglecting $\mathrm{Var}(T_2)$ leads to an explicit condition involving $X, l_\parallel, l_\perp$ and σ_ϵ:

$$X \ll A\left(\frac{l_\perp^4}{l_\parallel}\right)^{1/3}\sigma_\epsilon^{-2/3} \tag{30}$$

where A is defined as in the isotropic case by equation (16).

5. Conclusion

The new result of this paper is the calculation of the second-order term of the travel-time variance in random media. After a linear increase (first order or Chernov approximation), the travel-time variance explodes at a certain propagation distance due to the occurrence of the first caustics. This behaviour has been qualitatively and quantitatively validated with a numerical experiment based on ray tracing and the Gaussian beam summation method.

This theory is valid at second order, for applications in which the travel-time perturbation is only weakly nonlinear. Moreover, our results are valid in the geometrical optics approximation, when diffraction effects are negligible. The scattering phenomenon, which occurs at a certain propagation distance (see equation (3)), modifies the behaviour of the travel-time variance (Rytov *et al* [20]).

In this work, we have used a general form of the medium covariance which permits one to extract the standardized covariance, i.e. the canonical form of the covariance. This formulation makes the consideration of statistically anisotropic random media easier, and we have given a general formula for the mean and variance of the travel times. The same method would allow us to obtain expressions for the travel-time covariance (Iooss [10]) and the statistical moments of the amplitude.

Appendix A. Travel-time mean at second order

We calculate $\langle T_2 \rangle$ in the geometrical optics for a 3D plane wave, with the same approach as Boyse and Keller [3]. We have (see equation (7))

$$T_2(\boldsymbol{r}) = -\frac{1}{4c_0}\int_0^X \left[\int_0^{r'} \nabla_\perp \epsilon(r'', \boldsymbol{r}_\perp)\,\mathrm{d}r''\right]^2 \mathrm{d}r'. \tag{A1}$$

Taking the average value, we obtain

$$\begin{aligned}\langle T_2(\boldsymbol{r})\rangle &= -\frac{1}{4c_0}\int_0^X\int_0^{r'}\int_0^{r'} \langle \nabla_\perp\epsilon(r_1'', \boldsymbol{r}_\perp)\nabla_\perp\epsilon(r_2'', \boldsymbol{r}_\perp)\rangle\,\mathrm{d}r_1''\,\mathrm{d}r_2''\,\mathrm{d}r' \\ &= \frac{1}{4c_0}\int_0^X\int_0^{r'}\int_0^{r'} \nabla_\perp^2 C_\epsilon(r_1''-r_2'', \boldsymbol{r}_\perp)|_{r_\perp=0}\,\mathrm{d}r_1''\,\mathrm{d}r_2''\,\mathrm{d}r'\end{aligned} \tag{A2}$$

because $C_{\epsilon'}(\boldsymbol{r}) = -C''_\epsilon(\boldsymbol{r})$ (Papoulis [18]).

By using (9), we have

$$\nabla_\perp^2 C_\epsilon(X, \boldsymbol{r}_\perp)|_{r_\perp=0} = \frac{\sigma_\epsilon^2}{LX} N'\left(\frac{X}{L}\right). \tag{A3}$$

With the new variables $r'' = r_1'' - r_2''$ and $s = \frac{1}{2}(r_1'' + r_2'')$, equations (A2) and (A3) lead to

$$\langle T_2(\boldsymbol{r})\rangle = \frac{\sigma_\epsilon^2}{4c_0 L}\int_0^X\int_0^{r'}\int_0^\infty \frac{N'(r''/L)}{r''}\,\mathrm{d}r''\,\mathrm{d}s\,\mathrm{d}r'. \tag{A4}$$

We have extended the integration domain of r'' to infinity because $N'(r''/L)/r''$ is concentrated in the $|r''| < L$ domain, and we have assumed $X \gg L$ (equation (1)).

Finally, with a last variable change, we obtain from (A4)

$$\langle T_2(\boldsymbol{r})\rangle = \frac{\sigma_\epsilon^2}{8c_0}\frac{X^2}{L}\int_0^\infty \frac{N'(r')}{r'}\,\mathrm{d}r'. \tag{A5}$$

For a spherical wave (see equation (7)), we have to add $\frac{r_1''}{r'}\frac{r_2''}{r'}$ in the integrand of equation (A2). We obtain

$$\langle T_2(\boldsymbol{r})\rangle = \frac{\sigma_\epsilon^2}{4c_0L}\int_0^X\int_0^{r'}\int_0^{r'}\left(\frac{s^2}{r'^2}-\frac{r''^2}{4r'^2}\right)\frac{N'(r''/L)}{r''}\,\mathrm{d}r''\,\mathrm{d}s\,\mathrm{d}r'. \tag{A6}$$

As $N'(r''/L)/r''$ is concentrated in the $|r''| < L$ domain, the term with $\frac{r''^2}{4r'^2}$ has a negligible contribution to the integration. Keeping the other term, we finally obtain

$$\langle T_2(\boldsymbol{r})\rangle = \frac{1}{3}\frac{\sigma_\epsilon^2}{8c_0}\frac{X^2}{L}\int_0^\infty\frac{N'(r')}{r'}\,\mathrm{d}r'. \tag{A7}$$

The travel-time variance of a spherical wave is one third of that of a plane wave.

Appendix B. Travel-time variance at second order

We calculate $\mathrm{Var}(T_2) = \langle T_2^2\rangle - \langle T_2\rangle^2$ in the geometrical optics for a plane wave. From (A1), we have

$$\langle T_2^2(\boldsymbol{r})\rangle = \frac{1}{16c_0^2}\int_0^X\mathrm{d}r_1\int_0^{r_1}\mathrm{d}r_1'\int_0^{r_1}\mathrm{d}r_1''\int_0^X\mathrm{d}r_2\int_0^{r_2}\mathrm{d}r_2'\int_0^{r_2}\mathrm{d}r_2''$$
$$\times\langle\nabla_\perp\epsilon(r_1',\boldsymbol{r}_\perp)\nabla_\perp\epsilon(r_1'',\boldsymbol{r}_\perp)\nabla_\perp\epsilon(r_2',\boldsymbol{r}_\perp)\nabla_\perp\epsilon(r_2'',\boldsymbol{r}_\perp)\rangle. \tag{B1}$$

This expression contains the fourth moment of $\nabla_\perp\epsilon$. With the hypothesis of a Gaussian statistical distribution for ϵ, we have (Papoulis [18])

$$\begin{aligned}\langle\nabla\epsilon(x_1)\nabla\epsilon(x_2)\nabla\epsilon(x_3)\nabla\epsilon(x_4)\rangle &= \frac{\partial}{\partial x_1}\frac{\partial}{\partial x_2}\frac{\partial}{\partial x_3}\frac{\partial}{\partial x_4}\langle\epsilon(x_1)\epsilon(x_2)\epsilon(x_3)\epsilon(x_4)\rangle\\ &= \frac{\partial}{\partial x_1}\frac{\partial}{\partial x_2}\frac{\partial}{\partial x_3}\frac{\partial}{\partial x_4}[C_\epsilon(x_1-x_2)C_\epsilon(x_3-x_4)\\ &\quad + C_\epsilon(x_1-x_3)C_\epsilon(x_2-x_4)+C_\epsilon(x_1-x_4)C_\epsilon(x_2-x_3)].\end{aligned} \tag{B2}$$

We note $\Upsilon_\epsilon(h_1,h_2,\boldsymbol{r}_\perp) = \nabla_\perp^2 C_\epsilon(h_1,\boldsymbol{r}_\perp)\nabla_\perp^2 C_\epsilon(h_2,\boldsymbol{r}_\perp)$. With (A3), we obtain

$$\Upsilon_\epsilon(h_1,h_2,0) = \frac{\sigma_\epsilon^2}{L^2h_1h_2}N'\left(\frac{h_1}{L}\right)N'\left(\frac{h_2}{L}\right). \tag{B3}$$

Putting (B2) and (B3) in equation (B1), we obtain

$$\langle T_2^2(\boldsymbol{r})\rangle = \frac{1}{16c_0^2}\int_0^X\mathrm{d}r_1'\int_0^{r_1'}\mathrm{d}r_1''\int_0^{r_1'}\mathrm{d}r_1'''\int_0^X\mathrm{d}r_2'\int_0^{r_2'}\mathrm{d}r_2''\int_0^{r_2'}\mathrm{d}r_2'''$$
$$\times\Upsilon_\epsilon(r_1'-r_1'',r_2'-r_2'',0)+\Upsilon_\epsilon(r_1'-r_2',r_1''-r_2'',0)+\Upsilon_\epsilon(r_1'-r_2'',r_2'-r_1'',0). \tag{B4}$$

We simplify the three terms in the same manner as in appendix A. For example, for the first term, the variable changes are $h_1 = r_1'-r_1''$, $h_1' = \frac{1}{2}(r_1'+r_1'')$, $h_2 = r_2'-r_2''$, and $h_2' = \frac{1}{2}(r_2'+r_2'')$. By extending the integration domain of h_1' and h_2' to infinity, the three terms lead to the same result. Hence, we have

$$\langle T_2^2\rangle = \frac{3X^4}{64c_0^2}\frac{\sigma_\epsilon^4}{L^2}\int_0^\infty\int_0^\infty\frac{N'(h_1/L)N'(h_2/L)}{h_1h_2}\,\mathrm{d}h_1\,\mathrm{d}h_2. \tag{B5}$$

Finally, we have calculated the travel-time variance at second order of a plane wave:

$$\mathrm{Var}(T_2) = \frac{X^4}{32c_0^2}\frac{\sigma_\epsilon^4}{L^2}\left[\int_0^\infty \frac{N'(u)}{u}\,\mathrm{d}u\right]^2\,\mathrm{d}u. \tag{B6}$$

By the same arguments as in appendix A, the travel-time variance of a spherical wave is $\frac{1}{9}$ of that of a plane wave.

Appendix C. Geometrical anisotropy in 3D

For three-dimensional random media, expressions are more complex than in 2D. Let (l_1, l_2, l_3) be the correlation lengths in a $(\boldsymbol{e}_1, \boldsymbol{e}_2, \boldsymbol{e}_3)$ orthogonal basis, and the matrix

$$\boldsymbol{\Lambda} = \left(\frac{1}{l_1^2}, \frac{1}{l_2^2}, \frac{1}{l_3^2}\right)\boldsymbol{I}_3$$

with $\boldsymbol{I}_3$ the 3D identity matrix. The $(\boldsymbol{e}_1, \boldsymbol{e}_2, \boldsymbol{e}_3)$ basis is defined by a 3D rotation of the $(Ox, Oy, Oz) = (h_1, h_2, h_3)$ initial Cartesian basis, which involves three elementary rotations of angles $\theta_1, \theta_2, \theta_3$ (see Wackernagel [26]). The rotation matrix $\boldsymbol{Q}$ is written as

$$\boldsymbol{Q} = \begin{pmatrix} \cos\theta_3 & \sin\theta_3 & 0 \\ -\sin\theta_3 & \cos\theta_3 & 0 \\ 0 & 0 & 1 \end{pmatrix}\begin{pmatrix} 1 & 0 & 0 \\ \cos\theta_2 & \sin\theta_2 & 0 \\ -\sin\theta_2 & \cos\theta_2 & 0 \end{pmatrix}\begin{pmatrix} \cos\theta_1 & \sin\theta_1 & 0 \\ -\sin\theta_1 & \cos\theta_1 & 0 \\ 0 & 0 & 1 \end{pmatrix}. \tag{C1}$$

The propagation direction of the wave is defined by the azimuthal angle α_1 in the (e_1, e_2) basis, and the polar angle α_2 (with e_3). Therefore, we call the propagation vector $\boldsymbol{d}_\parallel$ and the transverse vectors $\boldsymbol{d}_{\perp 1}$ and $\boldsymbol{d}_{\perp 2}$. We choose the orthogonal basis $(\boldsymbol{d}_\parallel, \boldsymbol{d}_{\perp 1}, \boldsymbol{d}_{\perp 2})$ with $\boldsymbol{d}_{\perp 1}$ in the vertical plane (including e_3) which forms an angle α_1 with e_1:

$$\boldsymbol{d}_\parallel = \begin{pmatrix} \cos\alpha_1 \sin\alpha_2 \\ \sin\alpha_1 \sin\alpha_2 \\ \cos\alpha_2 \end{pmatrix} \qquad \boldsymbol{d}_{\perp 1} = \begin{pmatrix} -\cos\alpha_1\cos\alpha_2 \\ -\sin\alpha_1\cos\alpha_2 \\ \sin\alpha_2 \end{pmatrix} \qquad \boldsymbol{d}_{\perp 2} = \begin{pmatrix} \sin\alpha_1 \\ -\cos\alpha_1 \\ 0 \end{pmatrix} \tag{C2}$$

Let $\boldsymbol{h}$ be a vector, we define the standardized covariance N by

$$C_\epsilon(\boldsymbol{h}) = \sigma_\epsilon^2 N\big(\sqrt{\boldsymbol{h}^T\boldsymbol{Q}^T\boldsymbol{\Lambda}\boldsymbol{Q}\boldsymbol{h}}\big). \tag{C3}$$

Therefore, to find the correlation length in the wave propagation basis, let us replace $\boldsymbol{h}$ by $h\boldsymbol{d}_\parallel$, $h\boldsymbol{d}_{\perp 1}$ and $h\boldsymbol{d}_{\perp 2}$. For example, if $\boldsymbol{h}$ is oriented along the propagation direction,

$$C_\epsilon(\boldsymbol{h}) = \sigma_\epsilon^2 N\left(\frac{h}{l_\parallel}\right) = \sigma_\epsilon^2 N\big(h\sqrt{\boldsymbol{d}_\parallel^T\boldsymbol{Q}^T\boldsymbol{\Lambda}\boldsymbol{Q}\boldsymbol{d}_\parallel}\,\big).$$

We find

$$\frac{1}{l_\parallel^2} = \boldsymbol{d}_\parallel^T\boldsymbol{Q}^T\boldsymbol{\Lambda}\boldsymbol{Q}\boldsymbol{d}_\parallel \qquad \frac{1}{l_{\perp 1}^2} = \boldsymbol{d}_{\perp 1}^T\boldsymbol{Q}^T\boldsymbol{\Lambda}\boldsymbol{Q}\boldsymbol{d}_{\perp 1} \qquad \frac{1}{l_{\perp 2}^2} = \boldsymbol{d}_{\perp 2}^T\boldsymbol{Q}^T\boldsymbol{\Lambda}\boldsymbol{Q}\boldsymbol{d}_{\perp 2}. \tag{C4}$$

An important particular case of 3D anisotropic media is the transverse isotropic model: $l_{\perp 1} = l_{\perp 2} = l_\perp$. In the general case of a geometrical anisotropy, the formulae (27)–(30) remain valid by replacing $\frac{1}{l_\perp^2}$ with $\frac{1}{l_{\perp 1}^2} + \frac{1}{l_{\perp 2}^2}$ [10].

References

[1] Blanc-Benon P, Juvé D and Comte-Bellot G 1991 Occurence of caustics for high-frequency waves propagating through turbulent fields *Theor. Comput. Fluid Dynam.* **2** 271–8

[2] Blanc-Benon P, Juvé D, Ostashev V E and Wandelt R 1995 On the appearance of caustics for plane sound-wave propagation in moving random media *Waves Random Media* **5** 183–99

[3] Boyse W and Keller J B 1995 Short acoustic, electromagnetic and elastic waves in random media *J. Opt. Soc. Am.* **12** 380–9

[4] Cerveny V, Popov M M and Psencik I 1982 Computation of wave fields in inhomogeneous media—Gaussian beam approach *Geophys. J. R. Astron. Soc.* **70** 109–28

[5] Chernov L A 1960 *Wave Propagation in a Random Medium* (New York: McGraw-Hill)

[6] Fiorina D 1998 Application de la méthode de sommation de faisceaux Gaussiens à l'étude de la propagation ultrasonore en milieu turbulent *Thèse* École Centrale de Lyon

[7] Flatté S M, Dashen R, Munk W H, Watson K M and Zachariasen F 1979 *Sound Transmission throug a Fluctuating Ocean* (New York: Cambridge University Press)

[8] Flatté S M and Wu R S 1988 Small-scale structure in the lithosphere and asthenosphere deduced from arrival time and amplitude fluctuations at NORSAR *J. Geophys. Res.* **93** 6601–14

[9] Iooss B 1998 Seismic reflection traveltimes in two-dimensional statistically anisotropic random media *Geophys. J. Int.* **135** 999–1010

[10] Iooss B 1998 Tomographie statistique en sismique réflexion: estimation d'un modèle de vitesse stochastique *Thèse* Ecole des Mines de Paris

[11] Juvé D, Blanc-Benon P and Hugon-Jeannin Y 1991 Simulation numérique de la propagation en milieu aléatoire *Publ. LMA* **125** 245–55

[12] Karweit M and Blanc-Benon P 1993 Arrival-time variance for acoustic propagation in 3-D random media: the effect of lateral scale *C. R. Acad. Sci., Paris II* **316** 1695–702

[13] Karweit M, Blanc-Benon P, Juvé D and Comte-Bellot G 1991 Simulation of the propagation of an acoustic wave through a turbulent velocity field: a study of phase variance *J. Acoust. Soc. Am.* **89** 52–62

[14] Keller J B 1962 Wave propagation in random media *Symp. Applied Math.* vol 16 (Providence, RI: American Mathematical Society) pp 227–46

[15] Klyatskin V I 1993 Caustics in random media *Waves Random Media* **3** 93–100

[16] Kraichnan R H 1970 Diffusion by a random velocity field *Phys. Fluids* **13** 22–31

[17] Kulkarny V A and White B S 1982 Focusing of waves in turbulent inhomogeneous media *Phys. Fluids* **25** 1770–84

[18] Papoulis A 1965 *Probability, Random Variables and Stochastic Processes* (New York: McGraw-Hill)

[19] Roth M, Müller G and Snieder R 1993 Velocity shift in random media *Geophys. J. Int.* **115** 552–63

[20] Rytov S M, Kravstov Y A and Tatarskii V I 1987 *Principles of Statistical Radiophysics* (Berlin: Springer)

[21] Samuelides Y 1998 Velocity shift using the Rytov approximation *J. Acoust. Soc. Am.* **104** 2596–603

[22] Samuelides Y and Mukerji T 1998 Velocity shift in heterogeneous media with anisotropic spatial correlation *Geophys. J. Int.* **134** 778–86

[23] Shapiro S, Schwarz R and Gold N 1996 The effect of random isotropic inhomogeneities on the phase velocity of seismic waves *Geophys. J. Int.* **127** 783–94

[24] Snieder R and Aldridge D F 1995 Perturbation theory for travel times *J. Acoust. Soc. Am.* **98** 1565–9

[25] Tatarskii V I 1961 *Wave Propagation in a Turbulent Medium* (New York: Dover)

[26] Wackernagel H 1995 *Multivariate Geostatistics* (Berlin: Springer)

[27] Witte O, Roth M and Müller G 1996 Ray tracing in random media *Geophys. J. Int.* **124** 159–69